Phoenix Lander's Thermal Evolved Gas Analyzer (TEGA) Evolved Gas Hopping Mode Peak Maximum Reduced Data Record (EGH_PM_RDR): Data processing procedures to acquire evolved gas peak maximums from peak hopping mode datasets.

B. Sutter, A. Garcia, D. Hamara, P.D. Archer, P.B. Niles.

1. Introduction

The Phoenix Mars Scout lander mission investigated atmosphere and geology of the north polar region of Mars in 2008. The Phoenix lander's Thermal and Evolved-Gas Analyzer (TEGA) instrument assessed the gas composition of the martian atmosphere and evaluated the mineralogy of the martian soil. The TEGA instrument consisted of eight small ovens connected to a 4-channel magnetic sector mass spectrometer (Channel 1, 0.7-4 m/z, Channel 2, 7-35 m/z, Channel 3, 14-70 m/z, Channel 4, 28-140 m/z) (Boynton et al., 2001; 2009 Hoffman et al., 2008; Slavney et al., 2008; Hecht et al., 2009; Sutter et al., 2024). The ovens heated soil samples from ambient to 1000°C where the evolved gases (e.g., H_2O, CO_2, etc.) from thermal decomposition of volatile bearing mineral phases were analyzed by TEGA's mass spectrometer.

Evolved gas results originally published to the PDS consist of either sweep mode (EGSRDR) or peak hopping mode (EGHRDR) data sets. (Hoffman et al., 2008; Slaveny et al., 2008). The sweep mode consisted of increasing the mass spectrometer acceleration voltage in a stepwise manor to cover the entire evolved gas mass to charge (m/z) range over the 4 channels of the magnetic sector mass spectrometer. Sweep mode was used for assessing which gases were present but had low time resolution, as too much time was spent moving between m/z peaks where data is less useful. The peak hopping mode and, the focus of this document, adjusted the spectrometer ion acceleration voltages to "hop" from m/z peak top to the next m/z peak top of selected m/z values. The peak hopping mode permitted acquisition of peak data with higher time resolution. Instead of taking a single point at a peak, which can miss the actual peak if the mass spectrometer is slightly mis-tuned, peak-hopping mode performed "mini-sweeps" of 5-7 points. A function was fit to these points to determine the actual peak value which is used for data analysis. The problem with the peak hopping mode data sets originally provided to the PDS (EGHRDR) (Table 1) was that only the mini-sweep data (EGHRDR_COUNTS) were published, not the actual peak value which, which complicates the analysis of the TEGA evolved gas data sets (Figures. 1 and 2).

The peak hopping mode was employed because of imprecise mass spectrometer tuning. This imprecision meant that TEGA was unable to consistently collect single point peak maximums at a predetermined voltage and thus had to spend time ensuring the m/z peak count maximums were located for each m/z peak during sample analysis. Because each peak analyzed consisted of 5-7 points, the TEGA team had to be selective in which m/z values to analyze for a given sample because analyzing all possible TEGA m/z values (1 to 140 m/a) in a single analysis would result in a time resolution not sufficient to measure evolved gas releases. Mass spectrometers with superior tuning (e.g., Mars Science Laboratory's Sample Analysis at Mars Instrument) have exceptional on-peak (m/z) calibration that permit consistent on-peak data acquisition at a much faster rate and, are able to scan more m/z integers (e.g.,1 to 535 m/z) while maintaining adequate time resolution (Mahaffy et al., 2012) Despite this compromise of focusing on select gases anticipated to be evolved from the martian soil, the peak hopping mode permitted improved counting statistics and achieve sufficient time resolution.

The overall goal of this work was to provide *single* point peak maximum (PM) data sets that will allow the user to easily evaluate the TEGA evolved gas data sets as function of analysis time or oven temperature. The objective of this work was to 1). Describe the procedure employed to process the EGHRDR 5-to-7-point datasets into single point PM data sets (EGH_PM_RDR) and to 2.) Provide the EGH_PM_RDR datasets to the PDS that will enable easier examination of the TEGA evolved gas data sets.

Table 1. Representative example of how a single set of 7 hop point mini-sweep EGHRDR data for evolved CO_2 with associated mass and UTC time were originally placed on the PDS in 2008. The original 2008 EGHRDR PDS data are presented in single row in the order of UTC Time, mass (m/z), and counts, respectively, and then repeated for the next set of hop points. Data are stacked here for illustrative purposes only. Counts (y) versus masses (m/z) (x) were used in the fitting equations below to find the peak maximum data point (A_0).

UTC Date	2008-06-17						
UTC Times	T09:26:29.527	T09:26:29.582	T09:26:29.633	T09:26:29.683	T09:26:29.738	T09:26:29.789	T09:26:29.527
Mass (m/z) (x)	43.91369	43.93568	43.95868	43.98171	44.00477	44.02785	44.05095
Counts (y)	141	323	611	834	900	715	529

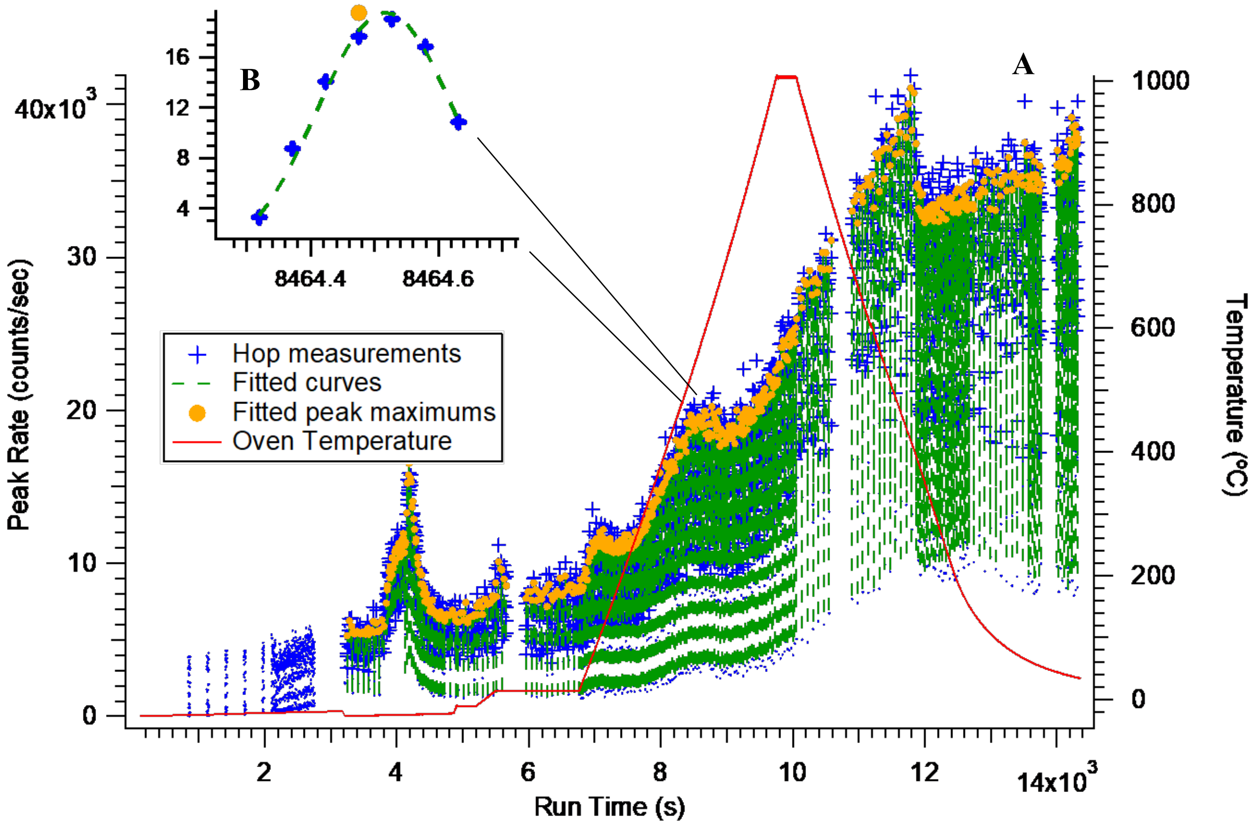

Figure 1. a) Evolved CO_2 (m/z44) versus time (sol 22, channel 4). Blue +, (mini-sweep hop measurements, EGHRDR), green ---, (fitted curves), and orange ● (peak maximums, PM). b) Inset of a subsample of mini-sweep 7 points and corresponding fitted curve and fitted peak maximum data point. Each orange point represents a single peak maximum associated with a set of 5 or 7 point mini-sweeps. The single peak maximums (orange points) were provided to the EGH_PM_RDR datasets.

2. Processing Peak Hoping Mode Data into Peak Maximum Points

The optimized single point peak maximum (PM) points (orange ●; Figures 1 and 2) were derived from each set of 5 or 7 points via mathematic fitting functions (e.g., Gaussian). For example, one peak maximum point (orange ●) was calculated from 7 points (blue +) by using a fitting function (green --) (Figure 2). This was repeated for the next set of 5 or 7 data points until a single data point versus time was produced over the entire time frame for each analyzed m/z (orange ●, Figure 1). The details of the coefficient values and equations used to initiate the optimized point calculation are available for each selected m/z in Table 3 and Figure. 2.

The PM data points (counts/s) (A_0) (see equations below) were calculated from the 5 to 7 point mini-sweeps via non-linear least squares analysis using either fit function 3 or 5 (listed below, Garcia et al., 2019). Function 3 was the dominant fitting function used while the presence of sloped tops in a few m/z values resulted in the use of function 5 (Table 3). The current fit functions labeled 3 and 5 were retained to maintain consistency with what was used internally by the TEGA team for data processing development. Fit functions 1 (simple line), 2 (quadratic) and 4 (n^{th}-order polynomial), were used for data processing testing purposes.

3) $y = A_0 e^{-\left(\frac{x-A_1}{A_2}\right)^{A_3}}$

This is the bell curve function.
y: 5-let or 7-hop data (CPS)
x: m/z of y
A_0: mass peak maximum ('*channel_mass*_CPS' column within '_cps_mass' file)
A_1: mass peak center
A_2: mass peak width
A_3: order of the fitted peak

5) $y = A_0 e^{-\left(\frac{x-A_1}{A_2}\right)^{A_3}} * \left(1 + A_4 * (x - A_1)\right)$

This is the bell slope function. This function allows the bell curve shape (fit function 3) to have a sloped top.
y: 5-let or 7- hop data (CPS)
x: m/z of y
A_0: mass peak maximum ('*channel_mass*_CPS' column within '_cps_mass' file)
A_1: mass peak center
A_2: mass peak width
A_3: order of the mass peak
A_4: slope of the top of the mass peak

The 5 or 7 hop data points (y) were fitted versus m/z (x) which consist of mass (m/z) data originally placed on the PDS (Table 3, Figure. 2). The PM (A_0) values were initialized using the most intense hop measurement and was allowed to vary resulting in the final PM value (A_0). The center_mass (A_1) defines where the center and where the most intense portion of the fitted peak should reside. A mass box value was assigned for each m/z value over which the fit function was valid (Table 3). Any hop measurements that fell outside this window that was centered on A_1 were ignored for the fit. A minimum of two data points were required to be present within the mass box for the fit to proceed. The A_2 coefficient defined the peak width. The A_2 coefficients were determined from the linear relationship of peak width versus mass from Mars atmospheric sweep data from sols 9 and 11 (Table 2) where:

$A_2 = W_0 + A_1 * W_1$

Table 2. Peak width table coefficients used to calculate mass peak width (A_2).

Channel	W_0	W_1
1	0.00000	0.02803
2	0.01277	0.007635
3	-0.00901	0.003923
4	0.00000	0.001511

Internal TEGA team documents state that the A_3 coefficient defined the order of the m/z peak. A_3 must be a positive, even integer (≥ 2) and held constant. A_3 is 2 for channel 4, 4 for channel 3 and channel 2, and 6 for channel 1. As A_3 increases, the sides of the bell curve become steeper, and the top of the bell curve becomes flatter. The coefficient A_4 defines the slope of the top of the peak for fit function 5. Only A_0 was allowed to vary while the coefficients A_1, A_2, A_3, and A_4 (Table 3) were not allowed to vary during the fit.

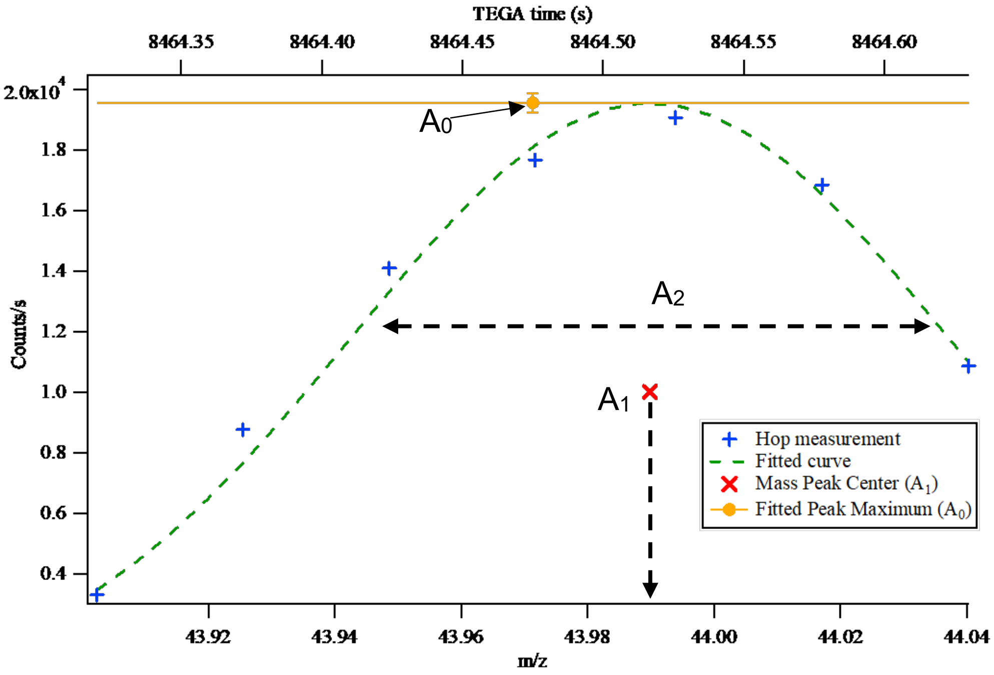

Figure 2. Example of evolved CO_2 (sol 22) single 7-hop point data versus m/z (bottom axis) and time (top axis). A_0: Fitted peak maximum, A_1: fitted peak center, A_2: fitted peak width.

Table 3. TEGA mass spectrometer channel and corresponding ion mass (*Channel_Mass*) analyzed by the TEGA evolved gas analyzer. *Ion* indicates the dominant ion of interest for a corresponding mass (m/z). Mass box and fit function coefficients are listed that were used to initiate calculation of the fitted peak maximum (A_0).

Channel_ Mass	Ion†	Fit Function	Mass Box (m/z)	Center Mass - A_1 (m/z)	Mass Peak Width - A_2 (m/z)	Mass Peak Order - A_3	Mass Peak Slope - A_4 (cps/(m/z))
1_1	^{1}H	5	0.0127	1.007825	0.02825	6	0.028652465
1_2	H_2, D	5	0.0254	2.0157	0.0565	6	-0.9
1_3	HD	5	0.0381	3.0219268	0.0847	6	0.085913379
2_12	^{12}C	3	0.047	12	0.10439	4	-
2_13	CH,^{13}C	3	0.0504	13.007825	0.11208	4	-
2_14	^{14}N	3	0.0539	14.00307	0.11968	4	-
2_15	^{15}N	3	0.0573	15.0001089	0.1273	4	-
2_27	C_2H_3	3	0.0986	27.023475	0.21909	4	-
2_28	N_2	3	0.102	28.00615	0.2266	4	-
3_15	CH_3	3	0.0225	15.023475	0.04993	4	-
3_16	CH_4 ,O	3	0.0242	16.01000	0.05388	4	-
3_17	OH	3	0.026	17.00274	0.0577	4	-
3_18	H_2O	5	0.0286	18.01056	0.0636	6	-0.6
3_19	^{18}OH	3	0.0295	19.00698	0.06556	4	-
3_20	$^{40}Ar^{++}$	3	0.0312	19.98119155	0.06938	4	-
3_27	C_2H_3	3	0.0437	27.023475	0.09701	4	-
3_28	N_2	5	0.0454	28.00615	0.10086	6	0.19
3_29	$^{14}N^{15}N$	3	0.0471	29.00318	0.10477	4	-
3_30	$C^{18}O$	3	0.0489	29.9991604	0.10868	4	-
3_32	O_2	3	0.0524	31.9898292	0.11649	4	-
3_39	C_3H_3	3	0.0648	39.023475	0.14408	4	-
3_40	^{40}Ar	3	0.0665	39.96239	0.14777	4	-
3_44	CO_2	3	0.0736	43.98983	0.16357	4	-
3_45	$^{13}CO_2$	3	0.0754	44.99318	0.1675	4	-
3_46	$C^{18}O^{16}O$	3	0.0771	45.99407	0.17143	4	-
3_55	C_4H_7	3	0.0931	55.054775	0.20697	4	-
3_56	C_4H_8	3	0.0949	56.0626	0.21093	4	-
4_29	^{13}CO	3	0.0351	28.9982694	0.04382	2	-
4_30	$C^{18}O$	3	0.0363	29.9991604	0.04533	2	-
4_32	O_2	3	0.0387	31.9898292	0.04834	2	-
4_34	^{34}S	3	0.0411	33.9678668	0.05133	2	-
4_35	Cl	3	0.0423	34.9688527	0.05284	2	-
4_39	C_3H_3	3	0.0472	39.023475	0.05896	2	-

Table 3 cont.

4_40	^{40}Ar	3	0.0483	39.96239	0.06038	2	-
4_41	C_3H_5	3	0.0496	41.039125	0.06201	2	-
4_44	CO_2	3	0.0532	43.98983	0.06647	2	-
4_45	$^{13}CO_2$	3	0.0544	44.99318	0.06798	2	-
4_46	$C^{18}O^{16}O$	3	0.0556	45.99407	0.0695	2	-
4_48	SO	3	0.058	47.9669853	0.07248	2	-
4_55	C_4H_7	3	0.0666	55.054775	0.08319	2	-
4_56	C_4H_8	3	0.0678	56.0626	0.08471	2	-
4_60	COS	3	0.0725	59.9669853	0.09061	2	-
4_64	SO_2	3	0.0773	63.9618999	0.09665	2	-
4_66	$^{34}SO_2$	3	0.0797	65.957696	0.09966	2	-
4_69	C_4H_5O	3	0.0834	69.0340396	0.10431	2	-
4_70	Cl_2	3	0.0845	69.9377054	0.10568	2	-
4_71	C_4H_7O	3	0.0859	71.0496896	0.10736	2	-
4_78	C_6H_6	3	0.0943	78.04695	0.11793	2	-
4_86	^{86}Kr	3	0.1038	85.91061401	0.12981	2	-
4_91	C_7H_7	3	0.1101	91.054775	0.13758	2	-
4_105	C_8H_9	3	0.127	105.070425	0.15876	2	-

†Some integer ion masses are identical as identified by Channel_Mass but are associated with different ions as their Mass Peak Center A_1 values differ slightly.

3. **Reporting Peak Maximum Data (A_0) (EGH_PM_RDR)**

The resulting peak maximum A_0 values are reported as counts per second (CPS) in the EGH_PM_RDR data file as '*channel_mass*_CPS'. Counts per second were calculated by dividing counts by the dwell time (milliseconds). Dwell time is found in the original EGH_RDR files (DWELL_TIME). The errors '*channel_mass*_CPS_SIGMA' were automatically calculated within fitting software to estimate the error of A_0. The error calculation assumes that the errors were normally distributed with zero mean and constant variance and that the fit function was a good description of the data. This assumption was not always valid and thus the *channel_mass*_CPS_SIGMA' values should be viewed as a minimum estimate of error. If the '*channel_mass*_CPS_SIGMA' was greater than 90% of the '*channel_mass*_CPS', then '*channel_mass*_CPS' value was not provided to the PDS. This was typically the case when the '*channel_mass*_CPS' values were very low.

The *channel_mass*_CPS (counts/seconds), '*channel_mass*_CPS_SIGMA' (counts/seconds) and instrument time ['*channel_mass*_TEGA_TIME' (milliseconds)] for all analyzed masses on a given sol were placed in a '*_mass_cps*' file on the PDS. The example presented in Table 4 shows the first 8 rows of data for channel 3_mass 16 (e.g., '3_16_TEGA_TIME', '3_16_CPS', and 3_16_CPS_SIGMA'). TEGA_TIME was derived from the median time of the 5- or 7-point hop measurements used for calculating the PM (A_0).

Along with the '_mass_cps' files, two more files were provided as a function of TEGA time (milliseconds): oven temperature ('_oven_temp') and the timing of the valving operations ('_valves'). Oven temperature will be important when combined with the evolved gas results to assess temperatures in which evolved gases were evolved during TEGA analyses. The TEGA instrument has many valves that are opened and closed during analyses and '_valves' file indicates which valve(s) were opened or closed at a given time by giving values of either 1 or 0, respectively. Figure 3 describes the valve locations relative to the mass spectrometer and oven.

Table 4. Representative example of the EGH_PM_RDR '_Mass_CPS' file for a soil analysis that reports the optimized peak maximum ('_CPS') (counts/second), corresponding error ('_CPS_SIGMA') and time ('_TEGA_TIME') (milliseconds) for a particular channel and mass.

3_16_TEGA_TIME	3_16_CPS	3_16_CPS_SIGMA
3318597	3413.17	130.906
3400668	3339.49	129.503
3482739	3345.45	129.649
3564810	3574.04	134.017
3646882	3258.37	127.988
3728953	3404.03	130.859
3811024	3361.5	130.021
3846098	3989.49	141.654

Table 5 provides a summary of all m/z and associated mass spectrometer channel (Channel_Mass) examined throughout the mission and indicates which m/z were examined on a particular sol. Depending on the objective of the analysis and what was and was not detected on previous analyses, the m/z analyzed varied between analyses. Mass spectrometer sensitivity degradation, particularly on channels 2 and 3, resulted in reduced detectability of m/z on those channels and m/z from those channels were not measured in later sols. See TEGA Sensitivity document for a description of changing mass spectrometer sensitivity throughout the mission.

Table 5 (next two pages). Color coded table describes what masses (m/z) and associated mass spectrometer channel (Channel_Mass) have calculated peak maximums data (EGH_PM_RDR) placed on the PDS for a particular sol. *Green* boxes indicate samples with available peak maximums data with counts >25 counts/s. *Yellow* indicates peak maximums with <25 counts/second to demonstrate which samples had extremely low counts/s. *Red* boxes indicate masses that were not selected to be analyzed. Wicked Witch 2 (WW2), Rosy Red 3b (RR3b) (Next page)

Table 5 *continued.*

		SAMPLE NAMES													
		Atmosphere (ATM)				Baby Bear				Wicked Witch					
		Sol													
		9	11	12	16	18	20	22	25	64	66	67	68	69	70
Channel_Mass	1_1	🟩	🟩	🟩	🟩	🟩	🟩	🟩	🟩	🟩	🟩	🟩	🟩	🟩	🟩
	1_2	🟩	🟩	🟩	🟩	🟩	🟩	🟩	🟩	🟩	🟩	🟩	🟩	🟩	🟩
	1_3	🟩	🟩	🟩	🟩	🟨	🟨	🟨	🟨	🟩	🟨	🟩	🟨	🟨	🟨
	2_12	🟩	🟩	🟩	🟩	🟨	🟨	🟨	🟨	🟥	🟥	🟥	🟥	🟥	🟥
	2_13	🟩	🟩	🟩	🟩	🟨	🟨	🟨	🟨	🟥	🟥	🟥	🟥	🟥	🟥
	2_14	🟩	🟩	🟩	🟩	🟩	🟩	🟩	🟩	🟥	🟥	🟥	🟥	🟥	🟥
	2_15	🟩	🟩	🟩	🟩	🟨	🟨	🟨	🟨	🟥	🟥	🟥	🟥	🟥	🟥
	2_27	🟩	🟩	🟩	🟩	🟨	🟨	🟨	🟨	🟥	🟥	🟥	🟥	🟥	🟥
	2_28	🟩	🟩	🟩	🟩	🟩	🟩	🟩	🟩	🟩	🟩	🟩	🟨	🟩	🟨
	3_15	🟥	🟥	🟥	🟥	🟥	🟥	🟥	🟥	🟩	🟩	🟩	🟩	🟩	🟩
	3_16	🟩	🟩	🟩	🟩	🟩	🟩	🟩	🟩	🟩	🟩	🟩	🟩	🟩	🟩
	3_17	🟩	🟩	🟩	🟩	🟩	🟩	🟩	🟩	🟩	🟩	🟩	🟩	🟩	🟩
	3_18	🟩	🟩	🟩	🟩	🟩	🟩	🟩	🟩	🟩	🟩	🟩	🟩	🟩	🟩
	3_19	🟩	🟩	🟩	🟩	🟩	🟩	🟩	🟩	🟨	🟨	🟩	🟨	🟩	🟨
	3_20	🟩	🟩	🟩	🟩	🟩	🟩	🟩	🟩	🟩	🟩	🟩	🟩	🟩	🟨
	3_27	🟩	🟩	🟩	🟩	🟩	🟩	🟩	🟩	🟥	🟥	🟥	🟥	🟥	🟥
	3_28	🟩	🟩	🟩	🟩	🟩	🟩	🟩	🟩	🟩	🟩	🟩	🟩	🟩	🟩
	3_29	🟩	🟩	🟩	🟩	🟩	🟩	🟩	🟩	🟩	🟩	🟩	🟩	🟩	🟩
	3_30	🟩	🟩	🟩	🟩	🟩	🟩	🟩	🟩	🟩	🟩	🟩	🟩	🟩	🟩
	3_32	🟩	🟩	🟩	🟩	🟩	🟩	🟩	🟩	🟩	🟩	🟩	🟩	🟩	🟩
	3_39	🟥	🟥	🟥	🟥	🟩	🟩	🟩	🟩	🟥	🟥	🟥	🟥	🟥	🟥
	3_40	🟩	🟩	🟩	🟩	🟩	🟩	🟩	🟩	🟩	🟩	🟩	🟩	🟩	🟩
	3_44	🟩	🟩	🟩	🟩	🟩	🟩	🟩	🟩	🟩	🟩	🟩	🟩	🟩	🟩
	3_45	🟩	🟩	🟩	🟩	🟩	🟩	🟩	🟩	🟩	🟩	🟩	🟩	🟩	🟨
	3_46	🟩	🟩	🟩	🟩	🟩	🟩	🟩	🟩	🟩	🟩	🟩	🟨	🟨	🟨
	3_55	🟥	🟥	🟥	🟥	🟨	🟨	🟨	🟨	🟥	🟥	🟥	🟥	🟥	🟥
	3_56	🟥	🟥	🟥	🟥	🟨	🟨	🟨	🟨	🟥	🟥	🟥	🟥	🟥	🟥
	4_29	🟥	🟥	🟥	🟥	🟥	🟥	🟥	🟥	🟩	🟩	🟩	🟩	🟥	🟩
	4_30	🟥	🟥	🟥	🟥	🟥	🟥	🟥	🟥	🟩	🟩	🟩	🟩	🟩	🟩
	4_32	🟥	🟥	🟥	🟥	🟥	🟥	🟥	🟥	🟩	🟨	🟩	🟩	🟩	🟩
	4_34	🟥	🟥	🟥	🟥	🟥	🟥	🟥	🟥	🟩	🟩	🟩	🟨	🟩	🟨
	4_35	🟥	🟥	🟥	🟥	🟥	🟥	🟥	🟥	🟨	🟨	🟩	🟨	🟩	🟨
	4_39	🟩	🟩	🟩	🟩	🟩	🟩	🟩	🟩	🟩	🟩	🟩	🟩	🟩	🟩
	4_40	🟩	🟩	🟩	🟩	🟩	🟩	🟩	🟩	🟩	🟩	🟩	🟩	🟩	🟩
	4_41	🟥	🟥	🟥	🟥	🟥	🟥	🟥	🟥	🟩	🟩	🟩	🟩	🟩	🟩
	4_44	🟩	🟩	🟩	🟩	🟩	🟩	🟩	🟩	🟩	🟩	🟩	🟩	🟩	🟩
	4_45	🟩	🟩	🟩	🟩	🟩	🟩	🟩	🟩	🟩	🟩	🟩	🟩	🟩	🟩
	4_46	🟩	🟩	🟩	🟩	🟩	🟩	🟩	🟩	🟩	🟩	🟩	🟩	🟩	🟩
	4_48	🟥	🟥	🟥	🟥	🟥	🟥	🟥	🟥	🟨	🟨	🟩	🟨	🟩	🟨
	4_55	🟥	🟥	🟥	🟥	🟥	🟩	🟩	🟩	🟩	🟩	🟩	🟩	🟩	🟩
	4_56	🟥	🟥	🟥	🟥	🟥	🟩	🟩	🟩	🟩	🟩	🟩	🟩	🟩	🟩
	4_60	🟥	🟥	🟥	🟥	🟥	🟥	🟥	🟥	🟩	🟩	🟩	🟨	🟩	🟨
	4_64	🟥	🟥	🟥	🟥	🟥	🟨	🟨	🟨	🟨	🟨	🟩	🟨	🟩	🟨
	4_66	🟥	🟥	🟥	🟥	🟥	🟨	🟨	🟨	🟨	🟨	🟩	🟨	🟩	🟨
	4_69	🟥	🟥	🟥	🟥	🟥	🟥	🟥	🟥	🟨	🟨	🟩	🟩	🟩	🟩
	4_70	🟥	🟥	🟥	🟥	🟥	🟥	🟥	🟥	🟨	🟨	🟩	🟨	🟩	🟨
	4_71	🟥	🟥	🟥	🟥	🟥	🟥	🟥	🟥	🟨	🟨	🟩	🟨	🟩	🟨
	4_78	🟥	🟥	🟥	🟥	🟥	🟩	🟥	🟩	🟩	🟩	🟩	🟩	🟩	🟩
	4_86	🟥	🟥	🟥	🟥	🟥	🟥	🟥	🟥	🟩	🟩	🟩	🟨	🟩	🟨
	4_91	🟥	🟥	🟥	🟥	🟥	🟨	🟥	🟥	🟥	🟥	🟩	🟥	🟩	🟥
	4_105	🟥	🟥	🟥	🟥	🟥	🟥	🟥	🟥	🟥	🟥	🟩	🟥	🟩	🟥

Table 5. *continued.*

		Sample Name													
		Rosy Red 3a			Burning Coals					WW2(Blank)		RR3b	ATM	RR3b	
		Sol													
		75	76	77	89	90	92	129	130	133	134	140	141	145	147
Channel_Mass	1_1	🟩	🟩	🟩	🟩	🟩	🟩	🟩	🟩	🟩	🟩	🟩	🟩	🟩	🟩
	1_2	🟩	🟩	🟩	🟩	🟩	🟩	🟩	🟩	🟩	🟩	🟩	🟩	🟩	🟩
	1_3	🟨	🟨	🟨	🟨	🟨	🟩	🟨	🟨	🟨	🟨	🟨	🟨	🟨	🟨
	2_12	🟥	🟥	🟥	🟥	🟥	🟥	🟥	🟥	🟥	🟥	🟥	🟥	🟥	🟥
	2_13	🟥	🟥	🟥	🟥	🟥	🟥	🟥	🟥	🟥	🟥	🟥	🟥	🟥	🟥
	2_14	🟥	🟥	🟥	🟥	🟥	🟥	🟥	🟥	🟥	🟥	🟥	🟥	🟥	🟥
	2_15	🟥	🟥	🟥	🟥	🟥	🟥	🟥	🟥	🟥	🟥	🟥	🟥	🟥	🟥
	2_27	🟥	🟥	🟥	🟥	🟥	🟥	🟥	🟥	🟥	🟥	🟥	🟥	🟥	🟥
	2_28	🟨	🟨	🟨	🟨	🟨	🟩	🟥	🟥	🟥	🟥	🟥	🟥	🟥	🟥
	3_15	🟩	🟩	🟩	🟩	🟩	🟥	🟥	🟥	🟥	🟥	🟥	🟥	🟥	🟥
	3_16	🟩	🟩	🟩	🟩	🟩	🟩	🟥	🟥	🟥	🟥	🟥	🟥	🟥	🟥
	3_17	🟩	🟩	🟩	🟩	🟩	🟩	🟥	🟥	🟥	🟥	🟥	🟥	🟥	🟥
	3_18	🟩	🟩	🟩	🟩	🟩	🟩	🟥	🟥	🟥	🟥	🟥	🟥	🟥	🟥
	3_19	🟨	🟩	🟩	🟩	🟩	🟩	🟥	🟥	🟥	🟥	🟥	🟥	🟥	🟥
	3_20	🟩	🟩	🟩	🟩	🟩	🟩	🟥	🟥	🟥	🟥	🟥	🟥	🟥	🟥
	3_27	🟥	🟥	🟥	🟥	🟥	🟥	🟥	🟥	🟥	🟥	🟥	🟥	🟥	🟥
	3_28	🟩	🟩	🟩	🟩	🟩	🟩	🟥	🟥	🟥	🟥	🟥	🟥	🟥	🟥
	3_29	🟩	🟩	🟩	🟩	🟩	🟩	🟥	🟥	🟥	🟥	🟥	🟥	🟥	🟥
	3_30	🟩	🟩	🟩	🟩	🟩	🟩	🟥	🟥	🟥	🟥	🟥	🟥	🟥	🟥
	3_32	🟩	🟩	🟩	🟩	🟩	🟩	🟥	🟥	🟥	🟥	🟥	🟥	🟥	🟥
	3_39	🟥	🟥	🟥	🟥	🟥	🟥	🟥	🟥	🟥	🟥	🟥	🟥	🟥	🟥
	3_40	🟩	🟩	🟩	🟩	🟩	🟩	🟥	🟥	🟥	🟥	🟥	🟥	🟥	🟥
	3_44	🟩	🟩	🟩	🟩	🟩	🟩	🟥	🟥	🟥	🟥	🟥	🟥	🟥	🟥
	3_45	🟩	🟩	🟩	🟩	🟩	🟨	🟥	🟥	🟥	🟥	🟥	🟥	🟥	🟥
	3_46	🟩	🟩	🟩	🟩	🟩	🟨	🟥	🟥	🟥	🟥	🟥	🟥	🟥	🟥
	3_55	🟥	🟥	🟥	🟥	🟥	🟥	🟥	🟥	🟥	🟥	🟥	🟥	🟥	🟥
	3_56	🟥	🟥	🟥	🟥	🟥	🟥	🟥	🟥	🟥	🟥	🟥	🟥	🟥	🟥
	4_29	🟩	🟩	🟩	🟩	🟩	🟩	🟥	🟥	🟥	🟥	🟥	🟥	🟥	🟥
	4_30	🟩	🟩	🟩	🟩	🟩	🟩	🟩	🟩	🟩	🟩	🟩	🟩	🟩	🟩
	4_32	🟩	🟩	🟩	🟩	🟩	🟩	🟩	🟩	🟩	🟩	🟩	🟩	🟩	🟩
	4_34	🟨	🟩	🟩	🟩	🟩	🟩	🟩	🟩	🟨	🟨	🟨	🟥	🟩	🟩
	4_35	🟨	🟨	🟨	🟨	🟨	🟩	🟨	🟨	🟨	🟨	🟨	🟥	🟨	🟨
	4_39	🟩	🟩	🟩	🟩	🟩	🟩	🟩	🟩	🟩	🟩	🟩	🟥	🟩	🟩
	4_40	🟩	🟩	🟩	🟩	🟩	🟩	🟩	🟩	🟩	🟩	🟩	🟩	🟩	🟩
	4_41	🟩	🟩	🟩	🟩	🟥	🟩	🟩	🟩	🟩	🟩	🟩	🟥	🟩	🟩
	4_44	🟩	🟩	🟩	🟩	🟩	🟩	🟩	🟩	🟩	🟩	🟩	🟩	🟩	🟩
	4_45	🟩	🟩	🟩	🟩	🟩	🟩	🟩	🟩	🟩	🟩	🟩	🟩	🟩	🟩
	4_46	🟩	🟩	🟩	🟩	🟩	🟩	🟩	🟩	🟩	🟩	🟩	🟩	🟩	🟩
	4_48	🟨	🟨	🟨	🟨	🟨	🟩	🟨	🟨	🟨	🟨	🟨	🟥	🟨	🟨
	4_55	🟩	🟩	🟩	🟩	🟩	🟩	🟩	🟩	🟩	🟩	🟩	🟥	🟩	🟩
	4_56	🟩	🟩	🟩	🟩	🟩	🟩	🟩	🟩	🟩	🟩	🟩	🟥	🟩	🟩
	4_60	🟩	🟨	🟩	🟩	🟩	🟩	🟩	🟩	🟩	🟩	🟩	🟥	🟩	🟩
	4_64	🟨	🟨	🟨	🟨	🟨	🟩	🟨	🟨	🟨	🟨	🟨	🟥	🟨	🟨
	4_66	🟨	🟨	🟩	🟨	🟨	🟩	🟨	🟨	🟨	🟨	🟨	🟥	🟨	🟨
	4_69	🟨	🟩	🟩	🟩	🟩	🟩	🟩	🟩	🟩	🟨	🟨	🟥	🟩	🟩
	4_70	🟨	🟨	🟩	🟨	🟨	🟩	🟨	🟨	🟨	🟨	🟨	🟥	🟨	🟨
	4_71	🟨	🟩	🟩	🟨	🟨	🟩	🟩	🟨	🟨	🟨	🟨	🟥	🟨	🟨
	4_78	🟩	🟩	🟩	🟩	🟩	🟩	🟩	🟩	🟩	🟨	🟨	🟥	🟩	🟩
	4_86	🟩	🟩	🟩	🟩	🟩	🟩	🟥	🟥	🟥	🟥	🟥	🟥	🟥	🟥
	4_91	🟨	🟥	🟩	🟥	🟩	🟩	🟩	🟨	🟨	🟨	🟨	🟥	🟨	🟩
	4_105	🟨	🟥	🟨	🟨	🟨	🟩	🟨	🟨	🟨	🟨	🟨	🟥	🟨	🟨

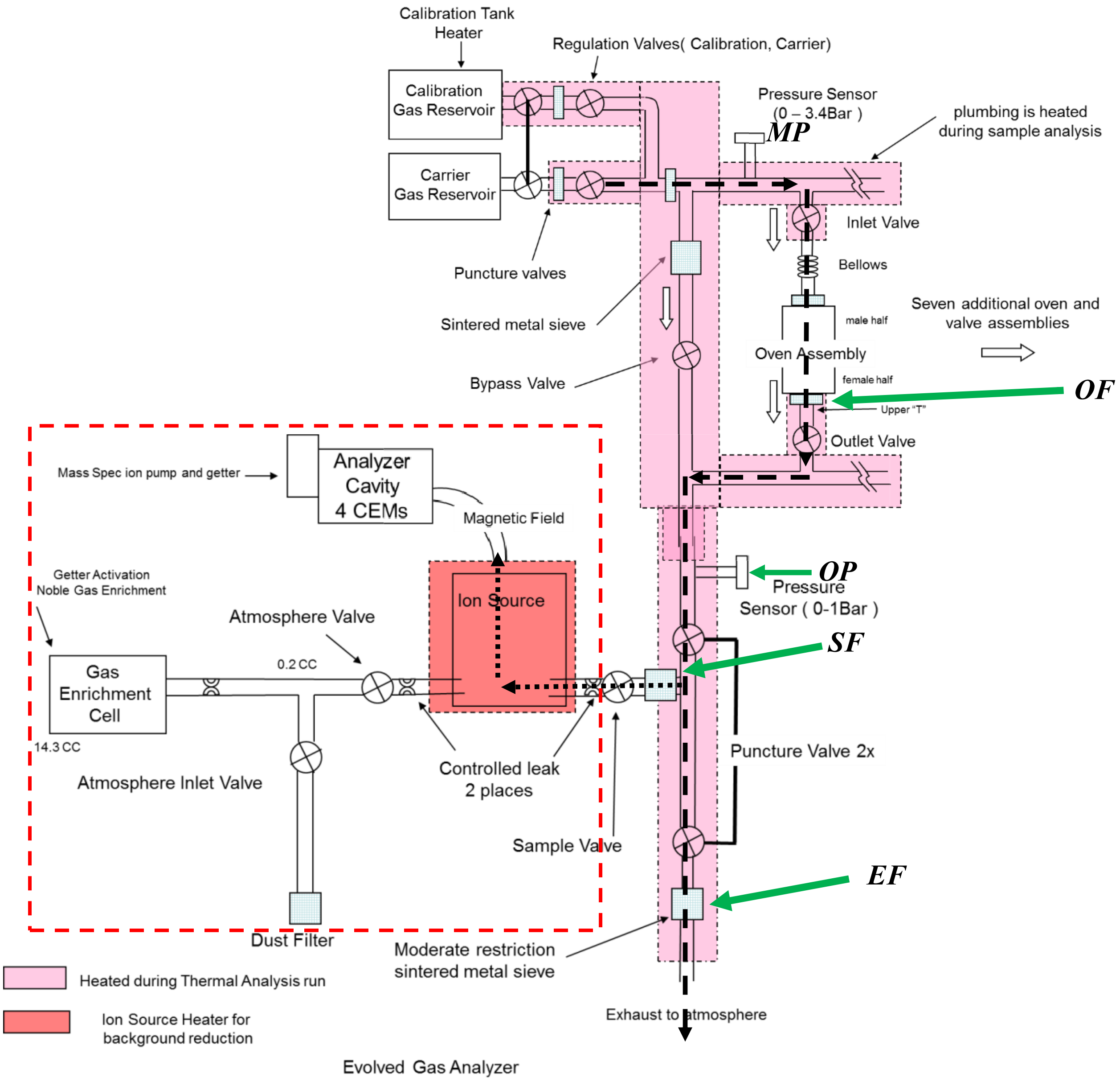

Figure 3. Schematic of the TEGA instrument indicating relative positions of valves, frits, pressure sensors, ovens, and mass spectrometer. Dashed lines with arrows indicate direction of carrier and evolved gas flow through the TEGA instrument during typical sample analyses. Most of the evolved gas was purged through the exhaust frit (*EF*). However, with the mass spectrometer pump activated and sample valve open, a portion of the sample evolved gas was analyzed by the mass spectrometer. Abbreviations, oven outlet frit (*OF*), manifold pressure sensor (*MP*), outlet pressure sensor (*OP*), sample frit (*SF*). Heavy red dashed line encloses mass spectrometer. (Sutter et al., 2024)

4. Deadtime Corrections

All mass spectrometer analyses of atmospheric gasses and evolved gases from soil were listed in the PDS as raw counts and have not been corrected for deadtime and background. The overall sensitivity of the instrument was also different for each channel utilized in the mass spectrometer. This was due to the performance of the channel electron multipliers used in each channel and how they degraded with time (Hoffman et al., 2009).

The deadtime in the counting system of the TEGA mass spectrometer was never well characterized and therefore remained somewhat difficult to quantify. Deadtime results from the loss of counts due to count "pile up" in the preamplifier-discriminator portion of the counting system. Niles et al. (2010) utilized a factory measurement made on the pre-amplifier after manufacture. However, this was not the only source of deadtime in the system and ideally the system should be characterized as a unit rather than by characterizing individual parts. Deadtime can be quantified according to this equation: $r = n*e^{-n\tau}$ where r is the measured counts/sec, n is the corrected counts/sec and τ is the deadtime of the system in nanosecs. The equation can be solved when the deadtime of the system is known or when the corrected count rate can be calculated via isotopic relationships. Niles et al. (2010) used a value of 71 ns for τ but did not identify an uncertainty on this value. Preliminary analysis suggests that this value could have as large an uncertainty as ±25 ns. Any isotope quantitative analysis using these numbers should account for that level of uncertainty in the correction. The data do not lend themselves to an obvious and uncontroversial deadtime correction method, thus isotope ratio and abundance calculations should be avoided where deadtime corrections could significantly impact the results. This could occur at count rates exceeding 100,000 cps.

Acknowledgments:

The authors are grateful to the engineers and scientists of the Mars 2007 Phoenix Scout's mission team, who made the mission possible and the reported data available. This work was funded by the Mars Data Analysis Program and the Internal Science Funding Model Mission-Enabling Research work package at Johnson Space Center. The authors gratefully acknowledge NASA Planetary Data System representatives Abigail Knight, Richard Chen, and Jennifer Ward and reviewers Heather Franz and Amy McAdam for useful comments and edits that significantly improved the data sets and documentation.

References

Boynton, W.V., Bailey, S.H., Hamara, D.K., Williams, M.S., Bode, R.C., Fitzgibbon, M.R. et al. (2001). Thermal and evolved gas analyzer: Part of the Mars Volatile and Climate Surveyor integrated payload. J. Geophys. Res. 106,17,683-17,698.

Boynton, W.V., Ming, D.W., Kounaves, S. P., Young, S. M. M., Arvidson, R. E., Hecht, M. H., et al. (2009). Evidence for calcium carbonate at the Mars Phoenix landing site. Science, 325, 61-64.

Garcia, A.H., Sutter, B., Archer, P.D., Niles, P.B, Stein, T.C., Boynton, W.V., Hamara, D. (2019). The 2008 MARS Phoenix Lander Thermal and Evolved Gas Analyzer (TEGA) dataset: Placing easily interpretable evolved gas data on the Planetary Data System (PDS). 50th Lunar Planet Sci. Conf. #1965 The Woodlands, TX March 18-22.

Hecht, M. H., Kounaves, S. P., Quinn, R. C., West, S. J., Young, S. M. M., Ming, D. W., et al. (2009). Detection of perchlorate and the soluble chemistry of Martian soil at the Phoenix Lander site. Science, 325, 64–67. https://doi.org/10.1126/science.1172466

Hoffman, J.H., Chaney, R.C., Hammack, H. 2008., Phoenix Mars Mission-The Thermal Evolved Gas Analyzer. J. Am. Soc. Mass Spectrom 19,1377-1383.

Mahaffy, P. R., Webster, C.R., Cabane, M., Conrad, P.G., Coll, P., Atreya, S.K., et al. (2012), The Sample Analysis at Mars investigation and instrument suite. Space Sci. Rev., 170, 401–478.

Niles, P.B., Boynton, W.V., Hoffman, J.H., Ming, D.W., & Hamara, D. (2010). Stable isotope measurements of Martian atmospheric CO2 at the Phoenix Landing site. Science, 329, 1334-1337.

Slavney, S., Crombie, M.K., Boynton, W.V., Tamppari, L., Arvidson, R.E., Grayzeck, E. 2008. TEGA Reduced Data Record Version 2.1. Planetary Data Service, Washington Univ.

Sutter B., Archer, P.D., Niles, P.B., Ming, D.W., Hamara, D., Boynton, W.V. 2024. Organic carbon and Ca-rich carbonate detections in soils of the Northern Plains, Mars: Evaluation of unpublished data interpretations from the Mars Phoenix Scout's, Thermal Evolved Gas Analyzer (TEGA). J. Geophys. Res., Planets, 129, e2024JE008335.
https://doi.org/10.1029/2024JE008335